



OPEN Influence of 3D printing angles on the accuracy of indirect adhesion transfer models: an in vitro study

Fangyong Zhu^{1,2}, Liuping Yu³, Meichun Hu³, Zhuang Ding¹, Hong Ma¹, Xingmei Feng², Yufeng Gao^{4,5}✉ & Yannan Cao^{1,5}✉

The aim of this study was to evaluate the effect of different Angle printing on the model on the printing platform and whether it affects the later transfer accuracy. Ten bracket transfer models were printed on the platform of the 3D printer in four ways: 0° without support rod, 0°, 45° and 90° with support rod. Transfer guide plates for transfer brackets were made using PVS. The linear and angular discrepancies were determined digitally by measuring six different dimensions. The best performance was achieved at 90° with a support bar, with mesioingival wing center point gap and diolingival wing center point gap of 0.169 and 0.176, respectively ($P < 0.05$). The linear deviation of groups A and B in the vertical direction was highest (0.285 ($P < 0.001$) and 0.283 ($P < 0.001$), respectively) when the transfer guide plate was made by PVS for the transfer bracket, followed by the proximal and distal direction. The best performance was achieved in the Orovestibular. The printing angle of the 3D indirect bonding slot transfer model on the printing platform significantly impacts the transfer accuracy, with the accuracy of the 45° and 90° bracket models having the least impact. A minimum transfer error of 90° since 90° 3D printed bracket transfer models with support rods have the best reliability.

Keywords 3D printing, Indirect bonding, Digital bonding, CAD/CAM, Polyvinyl siloxane

In the contemporary field of orthodontic treatment, the application of indirect bonding (IDB) trays, particularly those crafted from polyvinyl siloxane (PVS), playing a crucial role^{1–3}. These trays demonstrate outstanding performance in ensuring precise bracket positioning and effective transfer, not only enhancing treatment efficiency but also optimizing outcomes through accurate bracket placement. Although IDB trays made from PVS have shown good precision and consistency in pre-setting and transferring brackets on plaster models, ensuring that the preset bracket positions fully meet specific clinical requirements remains a challenge^{4,5}. This typically relies on the meticulous operations of experienced clinicians who make fine adjustments to minimize potential errors. Even with experienced professionals, completely avoiding errors in practical application is challenging, especially during the fabrication of IDB trays where slight displacements of bracket positions are common^{6–8}. Such minor displacements can significantly affect treatment outcomes. Therefore, continuous optimization of materials and techniques to improve the accuracy and predictability of treatments is crucial^{9–11}.

Additive manufacturing (additive manufacturing, AM), also known as 3D printing and rapid prototyping, is a technology that automatically creates personalized 3D objects by stacking them layer by layer based on CAD 3D models¹². Compared with other traditional production methods, 3D printing technology has many advantages such as high material utilization, shortened manufacturing time and cost¹³, and is widely used in dentistry and other fields.

Since Chaeles Hull proposed 3D printing, there have been 3D printing technologies such as selective laser sintering [ProMaker P1000 (France)], stereolithography [Form3 (USA)], selective laser melting [SLM280 (Germany)], digital light processing [RapidShape D40 (Germany)], direct metal laser sintering [DMP Flex350 (USA)], photopolymerization inkjet [StratasysJ750 (Israel)] and fusion deposition modeling [Raise3D (China)] and other 3D printing technology¹⁴. With the introduction and application of digital technologies such as digital scanning and Computer-Aided Design/Manufacturing (CAD/CAM), orthodontics is undergoing a technological revolution. These technologies not only enhance the precision of bracket placement but also allow for finer adjustments to brackets to meet the individual needs of patients, thereby advancing orthodontic treatments to a higher level^{15–17}. The application of CAD/CAM technologies and intraoral scanners has significantly increased

¹Department of Stomatology, Affiliated Hospital of Jiangnan University, 1000 Hefeng Road, Wuxi 214000, China.

²Department of Stomatology, Affiliated Hospital of Nantong University, Nantong 226001, China. ³Wuxi Medical College, Jiangnan University, Wuxi 214000, China. ⁴Jiangsu Wuxi People's Hospital, Wuxi 214000, China. ⁵Yufeng Gao and Yannan Cao contributed equally to this work. ✉email: 4645056@163.com; cyn525@163.com

the accuracy of bracket placement planning, substantially advancing the development of IDB technology^{18,19}. These technologies enable clinicians to precisely calculate and visualize the virtual positioning of brackets and the anticipated movement of teeth (including the roots) within a digital environment, optimizing treatment plans and enhancing outcomes^{20–22}. Specifically, clinicians can precisely plan the layout of brackets and buccal tubes based on the position of the tooth roots and materialize these designs through 3D printing, offering unprecedented design flexibility and manufacturing precision.

Polyvinyl siloxane (PVS) plays a pivotal role in this process, not only in the manufacturing of traditional IDB trays but also in ensuring two core elements of the trays: the precise planning of bracket positioning and the accuracy of their transfer. This high level of precision in positioning and transfer ensures the effectiveness and safety of orthodontic treatments, reducing the need for adjustments during treatment and discomfort for the patient.

In this study, we particularly emphasize the importance of utilizing 3D printing technology to precisely manufacture bracket transfer models. Choosing the appropriate printing angles is crucial for improving the accuracy and surface quality of the models, as it directly affects the performance of the final products. 3D printing technology not only simplifies the process of fine-tuning bracket positions but also addresses challenges inherent in traditional methods. Furthermore, this study will explore how printing angles impact the surface morphology of models and how these changes in surface morphology affect the accuracy of IDB trays and their acceptability in clinical settings. Through ongoing research and optimization of the design and manufacturing processes of IDB trays, we anticipate significant enhancements in the efficiency and effectiveness of orthodontic treatments, providing patients with more personalized and comfortable treatment options. The further development and application of these technologies suggest that orthodontic treatment is moving towards greater precision and personalization.

Materials and methods

This *in vitro* study was approved by the Medical Ethics Committee of the Affiliated Hospital of Jiangnan University in October 2022 (approval number: LS2022106). Confirm that all the experiments were performed in accordance with the relevant guidelines and regulations. Informed consent of the patient has been obtained (Fig. 1). Firstly, select a patient with periodontitis and acquire the digital impression of the maxillary dental arch. The inclusion criteria for this study were: (1) complete maxillary dentition, (2) normal tooth structure, (3) no orthodontic treatment history, (4) stable period of periodontitis. Exclusion criteria: (1) caries, (2) implant implantation, (3) poor oral hygiene, (4) dental deformities and quantitative defects, (5) severe tooth displacement hinders the placement of the tray.

Materials

The traditional metal bracket "Mini 0.022MBT (Protect Orthodontics Mini MBT 022 with hooks 5 to 5) Compatible (Protect Orthodontics MIM 1st) was selected for Molar Non-Convertible Tubes MBT 022) based on OrthoAnalyzer™ library (Fig. 2). The specific properties of the materials are shown in Table 1.

Digital imprinting

For the pre-treatment model selection in this study, a digital impression of the upper jaw of an elderly patient suffering from periodontal disease was chosen. The digital impression was captured and analyzed using OrthoAnalyzer™ software by 3Shape, based in Copenhagen, Denmark.

The preparation of bracket transfer models

The positioning of the bracket and buccal tube on the digital impression was determined based on the location of the tooth root in the CT scans. The bracket transfer model file was subsequently imported into the SHINING 3D™ printer software (AccuFab-L4D, Dental 3D Printer, China). Ten bracket transfer models were fabricated using four distinct methods: Group A (printed at 0° without support), Group B (printed at 0° with support), Group C (printed at 45°), and Group D (printed at 90°) as shown in Fig. 3.

The layer thickness for printing was set to 0.05 mm. Support structures were automatically generated, ensuring no contact points between the model and the 0.5 mm thick base plate. After the printing process was completed, the models were cleaned, and a specific resin program using a wavelength of 405 nm was employed for light-curing the models for 5 min. The finished transfer model is depicted in Fig. 4.

Accuracy analysis

Our experimental measurement method mainly used Medit T500 (Medit, Seoul, Korea) software. The software pre-designed the ideal bracket positioning on the virtual model, but there are deviations in the real bonding. We scanned the actual model onto the Medit T500 with our Reco CS3600 intraoral scanner, which has an accuracy of 20 μm, in order to measure the deviation from the virtual model. A technician used specialized software to identify the center points of the four wings of the bracket (mesiogingival wing, distal gingival wing, mesiogingival wing, and distal occlusion wing), as well as the center points of the buccal tube (mesiogingival wing and distal occlusion wing), the cusp traction hook, and the buccal tube traction hook. The discrepancies between these center points and the positions of the bracket and buccal tube identified in step 3 were subsequently calculated (Table 2; Figs. 5 and 6).

The preparation of PVS IDB guide

The PVS IDB guide was fabricated using transparent silicone rubber (Meijiayin®, Elastomeric Impression Material, China) as depicted in Fig. 4. Initially, the bottom of the tank was coated with Transbond™ XT (3M Unitek, USA). Subsequently, the trays were positioned on the model, and each bracket was subjected to photo-

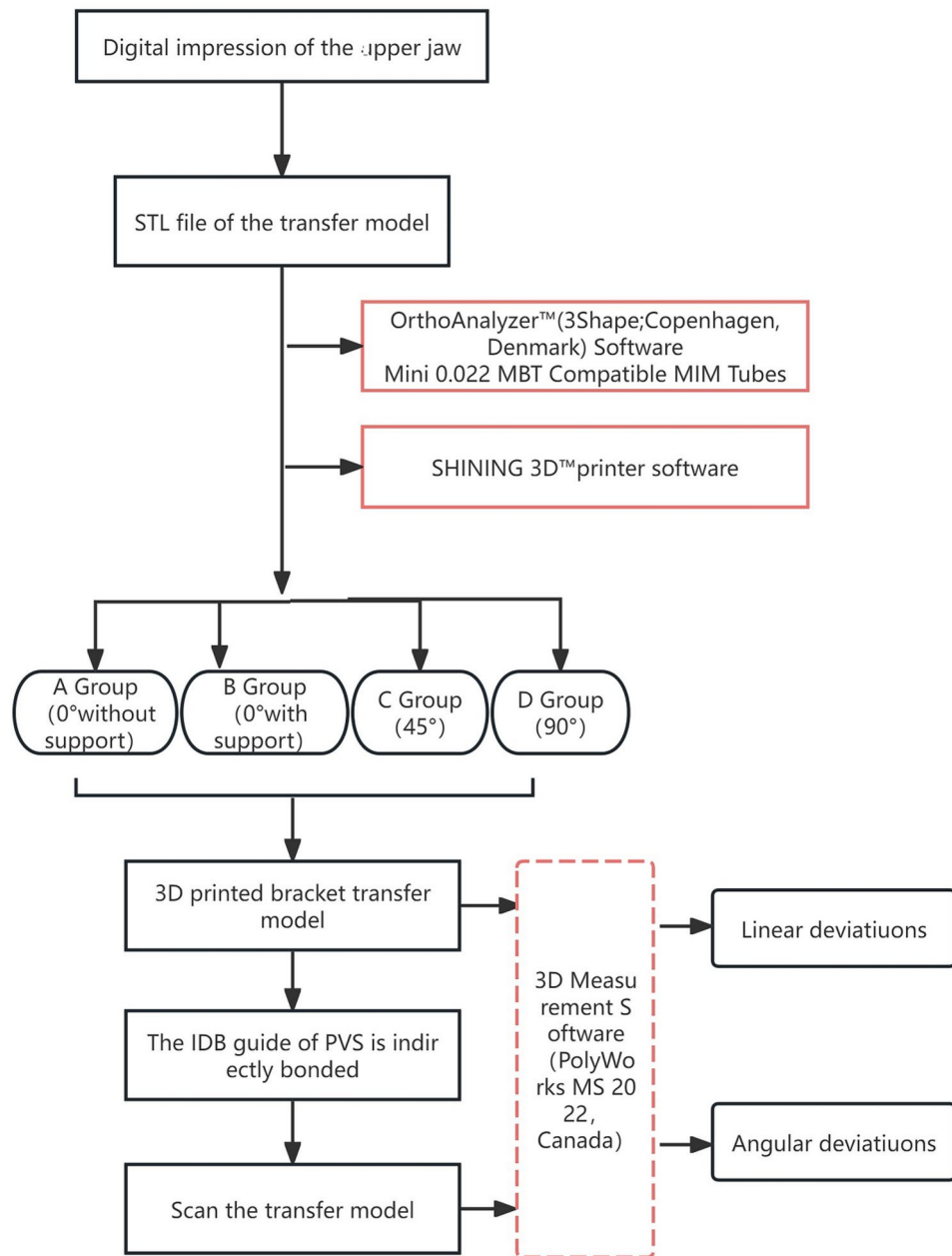


Fig. 1. shows the working flow chart of IDB made by PVS and the transfer accuracy flow of the position deviation of bracket.

curing for 10 s using an extra power photopolymerization mode while maintaining the trays in place with a slight and uniform biting pressure. After the IDB procedure, the tray was removed. A scalpel was utilized to make incisions from the edge of the bracket or tube towards the center, as shown in Fig. 4.

The analysis of bracket transfer models

To prevent reflection from the metal surface, scanning powder (metal-powder Dry White, R-dental Dentalerzeugnisse, Hamburg, Germany) was applied onto the model. Both pre- and post-bonding STL data were imported into 3D Measurement Software (PolyWorks MS 2022, Canada). Each tooth was removed and preserved both before and after bonding. In the image processing software, the corresponding teeth were aligned using local best-fit superimposition (Fig. 7). Cubic linear and cubic angular measurements were then performed for each bracket.

Statistical analysis

Continuous variables with a normal distribution were presented as means \pm standard deviation, whereas those with a non-normal distribution were reported as median [interquartile range (IQR)] (P25, P75). The overall

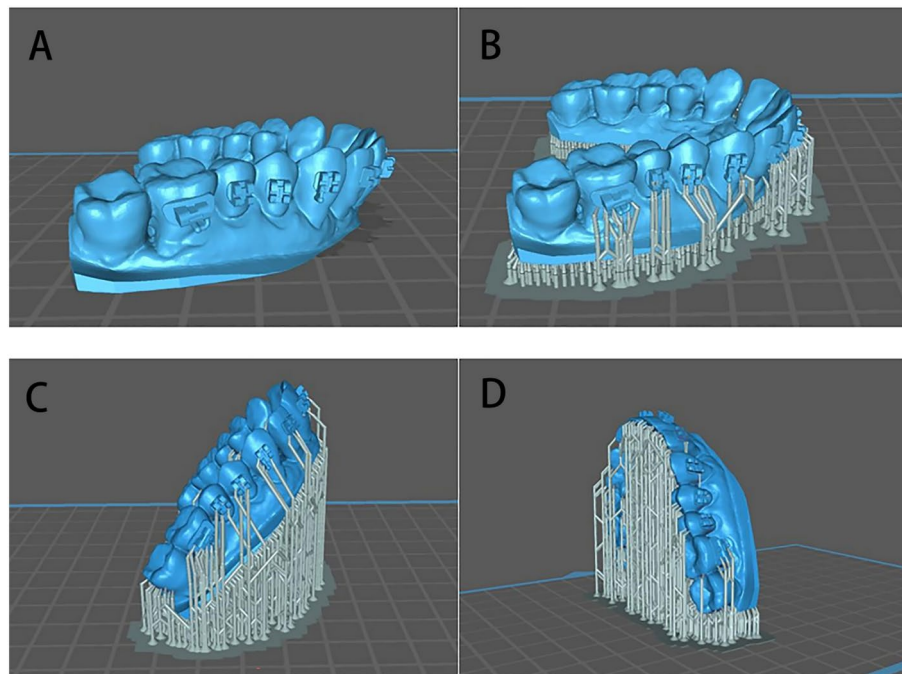


Fig. 2. SHINING 3D™ printer software was used to design group A (0° without support), Group B (0° with support), group C (45°) and group D (90°).

Performance	Numerical value	Testing standards
Hardness Shore D	77	ISO 868
Elastic modulus MPa	1021	ISO 527
Tensile strength MPa	27	ISO 527
Fracture elongation %	35	ISO 527
Bending modulus MPa	1429	ISO 178
Bending strength MPa	54	ISO 178

Table 1. Material properties.

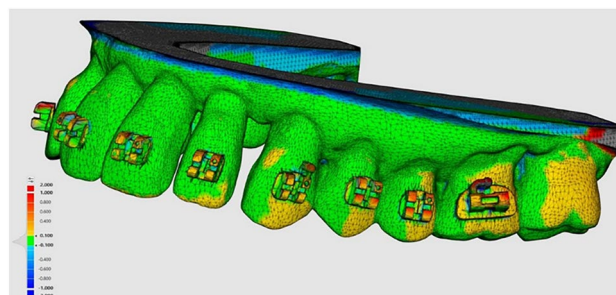


Fig. 3. Effect diagram of the unsupported bracket transfer model after 3D printing and superposition with the preoperative virtual model in 3D Measurement Software (PolyWorks MS 2022, Canada).

significant difference in transfer deviations between the four tooth groups (incisors, canines, premolars, molars) was assessed by the non-parametric Kruskal–Wallis H multipair comparison. Furthermore, the differences between the two transfer methods were determined using the Mann–Whitney test. The p -value < 0.05 was considered statistically significant. All statistical analyses were performed using SPSS v26.0.

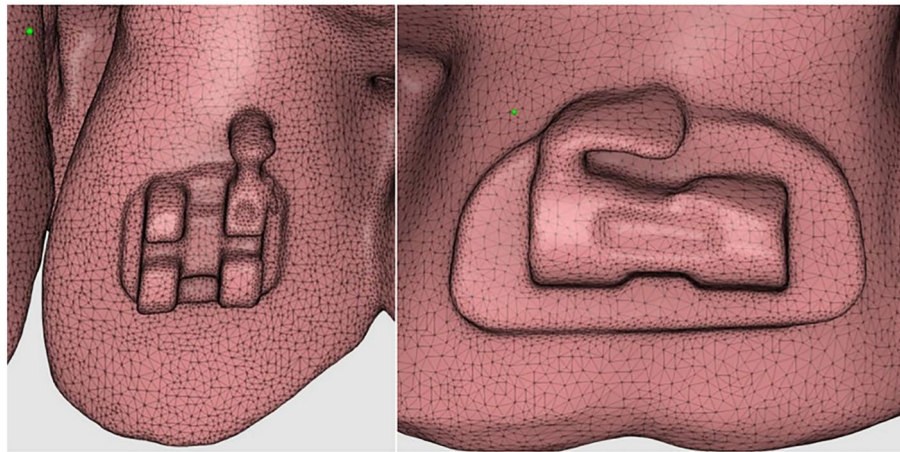


Fig. 4. Severely deformed traction hooks for the cusps and molars of the unsupported trusses transfer model in 3D Measurement Software (PolyWorks MS 2022, Canada).

Results

This study initially analyzed the printing accuracy of 400 brackets and 80 buccal tubes across four printing angles: 0° without supports, 0° with supports, 45° with supports, and 90° with supports, with each angle comprising 100 brackets and 20 buccal tubes. Post-printing deviations in the brackets and buccal tubes were observed to varying extents (Fig. 3). In Group A (0° without supports), a significant reduction in the dimensions of the four wings of the brackets was noted compared to the virtual model. The center point discrepancies for the mesial and distal gingival wings of the incisors were 0.257 ($P < 0.05$) and 0.262 ($P < 0.05$), respectively. Additionally, deformations were observed in the cusps and buccal tube traction hooks. The differences between the center points of each wing of the original design and the printed versions are detailed in Table 2. Notably, the accuracy improved with increasing printing plane angles, with the best performance observed at 90° with supports. The discrepancies in the center points of the mesial and distal gingival wings of the incisors at this angle were 0.169 ($P < 0.05$) and 0.176 ($P < 0.05$), respectively. Similar findings for other tooth positions were noted in Groups B, C, and D.

In the second part, transfer guide for the transfer bracket was made using PVS, followed by optical scanner scanning and digital planning of pre-bonding bracket position superposition. Each bracket produced three linear and three angular deviations. However, no group was shed during the transfer to the model. The transfer accuracy of 400 brackets and 80 buccal tubes was then measured. The linear deviations of groups A and B on incisor teeth were highest in the vertical direction (0.285 ($P < 0.001$) and 0.283 ($P < 0.001$), respectively), followed by the proximal and distal directions. The best performance was obtained in the Orovestibular. The largest angular deviation was in torque (0.910 in group A ($P < 0.05$) and 0.913 in group B ($P < 0.05$)). This difference was also reflected in the fangs, premolars, and molars. The accuracy improved with increasing print plane angle. Notably, the best performance was achieved at 90° with a support bar. Furthermore, the effect on tip and rotation was minimal (Table 3). The level of significance of differences between various dental types is shown in Table 3. Notably, IDB was not affected by different tooth surface morphology. Post hoc tests were performed to further analyze the differences for all significant groups. Hoffmann et al. found that three-dimensional printed trays achieved comparable results with the PVS trays in terms of bracket positioning accuracy. PVS showed significant differences between the tooth groups in all linear dimensions, Dreve exhibited a significant difference in the buccolingual direction only²³.

Discussion

This in vitro study aimed to determine whether the printing angle on the build platform affects the accuracy of bracket placement on the models. Additionally, the precision of bracket transfer using Polyvinyl Siloxane (PVS) transfer trays was also evaluated. The stair-step effect on the build platform significantly influenced accuracy, with a notable impact on the mesial and distal gingival wings of incisors as depicted in Fig. 5^{24,25}. Unkovskiy et al.²⁰ compared three different stereolithography (SLA) print orientations (0°, 45°, 90°) on a preset printer model and found that 45° yielded the best results²⁶. In our study, free-end support significantly impacted printing accuracy, necessitating different support structures to prevent detachment from the build platform during printing.

Compared to the virtual model, Group A, printed without supports, showed significant reductions in the dimensions of all four bracket wings. Moreover, the deviations of the mesial and distal gingival wings of brackets and buccal tubes were relatively large, primarily due to unsupported overhangs during printing. However, the deviations in the distal gingival wing of canines were relatively small, mainly due to the significant deviations in the canine traction hooks. Notably, accuracy improved with increasing print plane angles, with the best performance observed at 90° with supports. Shim et al.²⁷ found that printing at 90° was optimal for precision manufacturing, which aligns with our findings. The arrangement of models on the printer platform also affects accuracy. Arnold et al. found that the front of the platform could produce the most accurate models, whereas

Variables (Transfer errors)	n	Median (IQR)				Overall difference between tooth groups (P-values)	Pairwise comparisons (P-values)
		Without support (A)	Support (B)	Support 45° (C)	Support 90° (D)		
Incisors							
Mesiogingival wing center (mm)	20	0.257 (0.238–0.266)	0.170 (0.156–0.181)	0.171 (0.164–0.188)	0.169 (0.160–0.188)	<0.05	A/D: <0.05*; A/C: <0.05*;
Distal gingival wing center (mm)	20	0.262 (0.253–0.271)	0.185 (0.176–0.197)	0.168 (0.157–0.173)	0.176 (0.163–0.183)	<0.001	A/D: <0.05*; A/B: <0.001***; C/B: <0.05*;
Mesial wing center (mm)	20	0.180 (0.169–0.189)	0.179 (0.173–0.184)	0.171 (0.162–0.179)	0.172 (0.157–0.180)	<0.05	–
Distal wing center (mm)	20	0.184 (0.175–0.191)	0.173 (0.163–0.180)	0.161 (0.155–0.165)	0.157 (0.150–0.165)	<0.05	D/B: <0.05*; D/A: <0.001***; C/B: <0.05*; C/A: <0.001***;
Canines							
Mesiogingival wing center (mm)	20	0.191 (0.187–0.203)	0.187 (0.181–0.198)	0.173 (0.161–0.181)	0.172 (0.161–0.192)	<0.001	C/B: <0.05*; C/A: <0.05*; D/A: <0.05*;
Distal gingival wing center (mm)	20	0.187 (0.183–0.197)	0.194 (0.186–0.208)	0.173 (0.160–0.181)	0.167 (0.162–0.179)	<0.001	D/A: <0.001***; D/B: <0.001***; C/A: <0.05*; C/B: <0.001***; –
Mesial wing center (mm)	20	0.186 (0.182–0.195)	0.190 (0.185–0.198)	0.171 (0.166–0.183)	0.171 (0.159–0.178)	<0.001	D/A: <0.001***; D/B: <0.001***; C/A: <0.05*; C/B: <0.05*;
Distal wing center (mm)	20	0.186 (0.170–0.192)	0.180 (0.169–0.194)	0.169 (0.160–0.173)	0.160 (0.151–0.167)	<0.001	D/B: <0.05*; D/A: <0.001***; C/A: <0.05*;
Premolars							
Mesiogingival wing center (mm)	40	0.276 (0.265–0.286)	0.280 (0.274–0.292)	0.160 (0.153–0.164)	0.156 (0.150–0.163)	<0.001	D/A: <0.001***; D/B: <0.001***; C/A: <0.001***; C/B: <0.001***;
Distal gingival wing center (mm)	40	0.271 (0.263–0.282)	0.279 (0.267–0.288)	0.173 (0.158–0.180)	0.161 (0.155–0.168)	<0.001	D/C: <0.05*; D/A: <0.001***; D/B: <0.001***;
Mesial wing center (mm)	40	0.185 (0.181–0.192)	0.278 (0.268–0.288)	0.161 (0.156–0.168)	0.162 (0.153–0.166)	<0.001	D/B: <0.001***; D/A: <0.001***; C/A: <0.001***; C/B: <0.001***;
Distal wing center (mm)	40	0.184 (0.178–0.191)	0.175 (0.166–0.185)	0.174 (0.164–0.188)	0.176 (0.165–0.182)	<0.05	D/A: <0.05*; C/A: <0.05*;
Molars							
Mesio-central point (mm)	20	0.181 (0.177–0.190)	0.285 (0.279–0.290)	0.164 (0.159–0.167)	0.163 (0.158–0.170)	<0.001	C/A: <0.001***; C/B: <0.001***; D/A: <0.001***; D/B: <0.001***;
Distal central point (mm)	20	0.181 (0.171–0.187)	0.278 (0.270–0.286)	0.159 (0.154–0.166)	0.165 (0.159–0.171)	<0.001	C/A: <0.001***; C/B: <0.001***; D/A: <0.05*; D/B: <0.05*;
Continued							

Variables (Transfer errors)	n	Median (IQR)				Overall difference between tooth groups (P-values)	Pairwise comparisons (P-values)
		Without support (A)	Support (B)	Support 45° (C)	Support 90° (D)		
Cusp traction hook center point	20	0.383 (0.373–0.386)	0.180 (0.173–0.182)	0.154 (0.152–0.163)	0.158 (0.153–0.165)	<0.001	C/A: <0.001***; C/B: <0.001***; D/A: <0.001***; D/B: <0.001***;
Buccal tube traction hook center point	20	0.588 (0.582–0.593)	0.184 (0.179–0.189)	0.175 (0.170–0.183)	0.176 (0.164–0.185)	<0.05	C/A: <0.001***; D/A: <0.001***;

Table 2. The differences between the virtual model in group A, B, C and D after 3D printing for different tooth positions, four wings of the bracket and two center points of the buccal tube.* Significant difference ($P < 0.05$), ***Significant difference ($P < 0.001$).

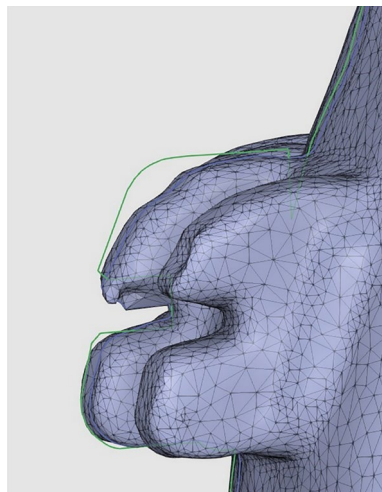


Fig. 5. Surface collapse of proximal and distal gingival wing of incisor in group A bracket transfer model caused by the ladder effect of the surface. The solid green line is the actual position of the design bracket.

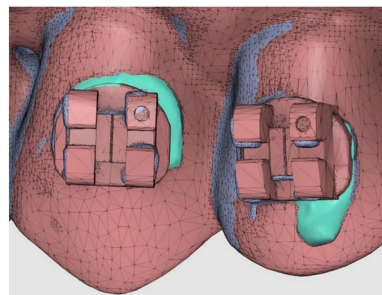


Fig. 6. Green shows the excess adhesive in 3D Measurement Software (PolyWorks MS 2022, Canada) after IDB production with PVS.

Unkovskiy et al. discovered that objects in the center of the build platform were more precise than those at the edges²⁸. In our study, the platform was centered, and then exposure time was moderately extended, resulting in a higher transfer accuracy of IDB trays made for PVS compared to other types in most studies²⁰. Schmid et al. reported that transfer accuracy of trays formed by a single vacuum was inferior to that of polydimethylsiloxane or double-layered IDB trays². However, it remains unclear whether errors on the printing platform affect transfer accuracy. In this study, classic IDB guides were made using PVS, with precise bracket and buccal tube placement planned based on the virtual positioning of tooth roots, followed by 3D printing. Yet, this method only provided a theoretical basis.

PVS was also used for the bracket transfer in all four model types. Additionally, a clinically acceptable range should be determined to assess the viability of this method. The American Association of Orthodontists

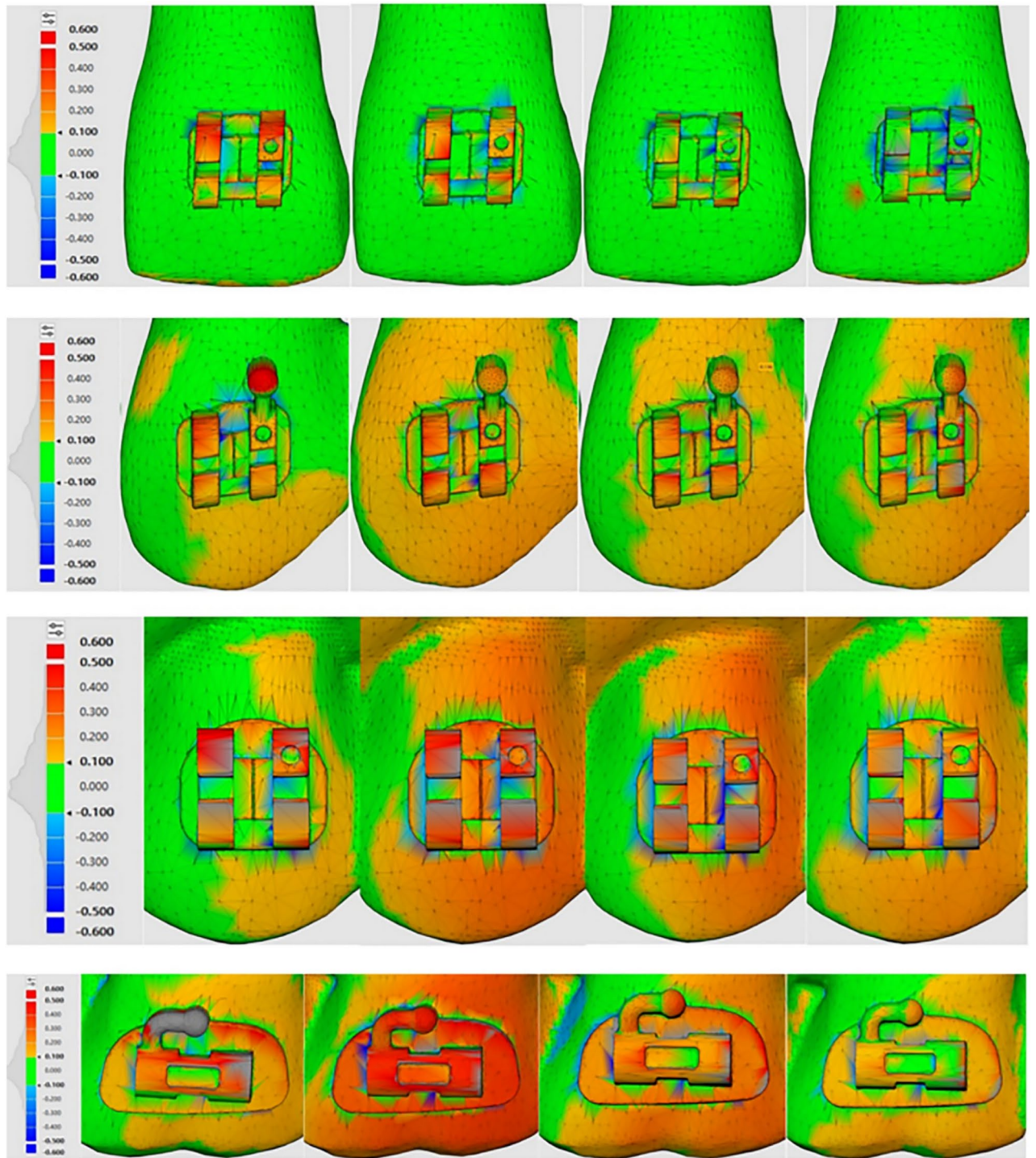


Fig. 7. The effect of group A, B, C and D's bracket transfer model after 3D printing and superimposed with the preoperative virtual model in 3D Measurement Software (PolyWorks MS 2022, Canada). Red and blue represent low overlap, with more green areas indicating higher overlap.

recommends a maximum deviation for bracket placement of 0.5 mm and 2° ²⁰. In our study, measured deviations were within this range. Furthermore, there was no significant difference in transfer accuracy between Groups C and D.

The curing material was a major factor affecting accuracy, as any excess bonding material could be forced into spaces around the bracket, affecting the precision of bracket placement (Fig. 6). Niu et al. found that the accuracy of angular dimensions, torque, rotation, and tipping was lower than that of linear dimensions, consistent with our findings. At each angle, torque transfer was the poorest, primarily due to excessive bonding material. Yet,

Variables (Transfer errors)	Incisors Median (IQR)				Overall difference between tooth groups (P-values)	Pairwise comparisons (P-values)
	A (N = 40)	B (N = 40)	C (N = 40)	D (N = 40)		
Mesiodistal (mm)	0.180 (0.168–0.186)	0.182 (0.175–0.187)	0.154 (0.122–0.178)	0.162 (0.178–0.185)	< 0.001	C/A: < 0.001***; C/B: < 0.001***; D/B: < 0.001***;
Vertical (mm)	0.285 (0.280–0.290)	0.283 (0.278–0.290)	0.173 (0.168–0.179)	0.177 (0.171–0.184)	< 0.001	C/B: < 0.001***; C/A: < 0.001***; D/B: < 0.001***; D/A: < 0.001***;
Orovestibular (mm)	0.185 (0.180–0.193)	0.185 (0.181–0.194)	0.185 (0.180–0.192)	0.184 (0.176–0.187)	0.321	–
Torque (°)	0.910 (0.866–0.972)	0.913 (0.873–0.954)	0.860 (0.796–0.929)	0.769 (0.674–0.822)	< 0.05	D/A: < 0.001***; D/B: < 0.001***; C/A: < 0.05*; C/B: < 0.05*;
Rotation (°)	0.835 (0.802–0.894)	0.801 (0.736–0.858)	0.798 (0.713–0.841)	0.798 (0.715–0.837)	< 0.05	C/A: < 0.05*; D/A: < 0.05*;
Tip (°)	0.753 (0.689–0.797)	0.741 (0.697–0.770)	0.715 (0.650–0.755)	0.724 (0.661–0.781)	–	–
Variables (Transfer errors)	Canines Median (IQR)				Overall difference between tooth groups (P-values)	Pairwise comparisons (P-values)
	A (N = 20)	B (N = 20)	C (N = 20)	D (N = 20)		
Mesiodistal (mm)	0.185 (0.173–0.196)	0.184 (0.181–0.191)	0.150 (0.132–0.167)	0.148 (0.140–0.160)	< 0.001	D/B: < 0.001***; D/A: < 0.001***; C/A: < 0.001***; C/B: < 0.001***;
Vertical (mm)	0.189 (0.184–0.194)	0.186 (0.181–0.192)	0.180 (0.173–0.183)	0.175 (0.168–0.184)	< 0.001	D/A: < 0.001***; D/B: < 0.05*; C/A: < 0.05*;
Orovestibular (mm)	0.187 (0.179–0.192)	0.186 (0.182–0.189)	0.177 (0.163–0.185)	0.176 (0.172–0.183)	< 0.05	D/B: < 0.05*; D/A: < 0.05*; C/A: < 0.05*;
Torque (°)	0.901 (0.872–0.956)	0.899 (0.865–0.951)	0.818 (0.785–0.865)	0.836 (0.795–0.864)	< 0.001	D/B: < 0.001***; D/A: < 0.001***; C/A: < 0.001***; C/B: < 0.001***;
Rotation (°)	0.822 (0.774–0.891)	0.807 (0.739–0.898)	0.766 (0.717–0.811)	0.755 (0.689–0.799)	< 0.05	D/A: < 0.05*;
Tip (°)	0.827 (0.783–0.870)	0.813 (0.754–0.855)	0.779 (0.703–0.851)	0.738 (0.682–0.835)	< 0.05	–
Variables (Transfer errors)	Premolars Median (IQR)				Overall difference between tooth groups (P-values)	Pairwise comparisons (P-values)
	A (N = 40)	B (N = 40)	C (N = 40)	D (N = 40)		
Mesiodistal (mm)	0.185 (0.177–0.193)	0.185 (0.177–0.191)	0.177 (0.168–0.185)	0.171 (0.163–0.182)	< 0.001	D/A: < 0.001***; D/B: < 0.05*; C/A: < 0.05*; C/B: < 0.05*;
Vertical (mm)	0.287 (0.282–0.294)	0.288 (0.281–0.293)	0.178 (0.169–0.182)	0.179 (0.175–0.186)	< 0.001	D/B: < 0.001***; D/A: < 0.001***; C/A: < 0.001***; C/B: < 0.001***;
Orovestibular (mm)	0.173 (0.162–0.183)	0.180 (0.172–0.185)	0.168 (0.158–0.175)	0.173 (0.159–0.180)	< 0.05	C/B: < 0.001***; D/B: < 0.05*;
Torque (°)	0.910 (0.855–0.960)	0.903 (0.867–0.943)	0.829 (0.798–0.877)	0.837 (0.797–0.883)	< 0.001	C/A: < 0.001***; C/B: < 0.001***; D/B: < 0.001***; D/A: < 0.05*;
Rotation (°)	0.844 (0.780–0.922)	0.847 (0.815–0.884)	0.773 (0.750–0.856)	0.789 (0.756–0.859)	< 0.05	C/A: < 0.05*; C/B: < 0.05*; D/B: < 0.05*;
Tip (°)	0.812 (0.788–0.882)	0.820 (0.775–0.858)	0.800 (0.767–0.845)	0.790 (0.756–0.839)	–	–

Variables (Transfer errors)	Molars Median (IQR)				Overall difference between tooth groups (P-values)	Pairwise Comparisons (P-values)
	A (N = 20)	B (N = 20)	C (N = 20)	D (N = 20)		
Mesiodistal (mm)	0.189 (0.180–0.190)	0.188 (0.176–0.195)	0.171 (0.167–0.184)	0.176 (0.172–0.181)	< 0.001	C/B: < 0.05*; C/A: < 0.05*; D/B: < 0.05*; D/A: < 0.05*;
Vertical (mm)	0.288 (0.286–0.294)	0.287 (0.280–0.292)	0.175 (0.167–0.179)	0.172 (0.164–0.183)	< 0.001	C/B: < 0.001***; C/A: < 0.001***; D/B: < 0.001***; D/A: < 0.001***;
Orovestibular (mm)	0.190 (0.178–0.199)	0.178 (0.173–0.192)	0.172 (0.168–0.188)	0.173 (0.169–0.185)	< 0.05	C/A: < 0.05*; D/A: < 0.05*;
Torque (°)	0.893 (0.857–0.946)	0.859 (0.833–0.900)	0.798 (0.738–0.809)	0.809 (0.799–0.852)	< 0.001	C/B: < 0.05*; C/A: < 0.001***; D/A: < 0.001***;
Rotation (°)	0.836 (0.756–0.873)	0.860 (0.772–0.890)	0.786 (0.743–0.799)	0.753 (0.684–0.780)	< 0.05	D/A: < 0.05*; D/B: < 0.05*;
Tip (°)	0.817 (0.768–0.880)	0.803 (0.756–0.864)	0.771 (0.737–0.804)	0.768 (0.753–0.812)	–	–

Table 3. Differences between four groups (central incisor, cusp, first premolar, and first molar) brackets and preoperative virtual models were superimposed in 3D Measurement Software (PolyWorks MS 2022, Canada) after IDB was made using PVS.* Significant difference ($P < 0.05$), ***Significant difference ($P < 0.001$)

most studies lack an explanation for these results. Moreover, increasing the thickness of the silicone rubber and coordinating four-handed care was highly beneficial.

In this study, tooth morphology did not significantly affect transfer accuracy, likely due to the elasticity of PVS. Castilla et al.²⁸ explained that variations in guide thickness could lead to different results in arch accuracy, suggesting that differences in crown lengths between incisors and molars could affect guide thickness. When models are accurate, PVS transfer becomes more meaningful.

For this study, the PVS trays included the first molars, and the same upper jaw model was chosen for consistency. Various clinical challenges of IDBs, such as crowding, tooth rotation, and spacing, were also included in this analysis. However, in vitro studies lack the soft tissues present in in vivo studies, and the trays and brackets cannot move gingival tissue to achieve correct bracket placement. Furthermore, common clinical challenges such as saliva, muscle activity, oral restrictions, and patient cooperation were not considered. The post-curing process and its impact on the mechanical integrity of the IDB tray, considering the sustainability in clinical application, discussing the relationship between the support structure density and material loss, whether the curing technology or material variability will also affect the accuracy remains to be further studied.

Conclusion

PVS can be used to make the classic IDB guide plate. Besides, the 90° model provides the least linear and angular transfer errors. The 3D printed bracket transfer model of 90 with support rod has the best reliability in clinical use. However, in vivo studies are needed to confirm the accuracy of the clinical results.

Data availability

The datasets generated and analyzed during the current study are available from the corresponding author on reasonable request.

Received: 25 June 2024; Accepted: 12 February 2025

Published online: 15 March 2025

References

- Chaudhary, V. et al. A comparative assessment of transfer accuracy of two indirect bonding techniques in patients undergoing fixed mechanotherapy: A randomised clinical trial. *J. Orthod.* **48**(1), 13–23 (2021).
- Schmid, J. et al. Transfer accuracy of two indirect bonding techniques—an in vitro study with 3D scanned models. *Eur. J. Orthod.* **40**(5), 549–555 (2018).
- Zhang, Y. et al. Comparison of three-dimensional printing guides and double-layer guide plates in accurate bracket placement. *BMC Oral Health* **20**(1), 127 (2020).
- Faus-Matoses, I. et al. A novel digital technique for measuring the accuracy of an indirect bonding technique using fixed buccal multibracket appliances. *J. Personal. Med.* **11**(9), 932 (2021).
- Mujagic, M. et al. The herbst appliance combined with a completely customized lingual appliance: a retrospective cohort study of clinical outcomes using the american board of orthodontics objective grading system. *Int. Orthod.* **18**(4), 732–738 (2020).
- Pamukcu, H. & Özsoy, Ö. P. Indirect bonding revisited. *Turk. J. Orthod.* **29**(3), 80–86 (2016).
- Nawrocka, A. & Lukomska-Szymanska, M. The indirect bonding technique in orthodontics—a narrative literature review. *Materials (Basel)* **13**(4), 986 (2020).

8. Niu, Y., Zeng, Y., Zhang, Z., Xu, W. & Xiao, L. Comparison of the transfer accuracy of two digital indirect bonding trays for labial bracket bonding. *Angle Orthod.* **91**(1), 67–73 (2021).
9. von Glasenapp, J., Hofmann, E., Süpple, J., Jost-Brinkmann, P. G. & Koch, P. J. Comparison of two 3D-printed indirect bonding (IDB) tray design versions and their influence on the transfer accuracy. *J. Clin. Med.* **11**(5), 1295 (2022).
10. Süpple, J., von Glasenapp, J., Hofmann, E., Jost-Brinkmann, P. G. & Koch, P. J. Accurate bracket placement with an indirect bonding method using digitally designed transfer models printed in different orientations—an in vitro study. *J. Clin. Med.* **10**(9), 2002 (2021).
11. Koch, P. J., Albrecht, M., Lin, W. C. & Jost-Brinkmann, P. G. Accuracy of indirect bonding trays—A measurement algorithm. *Int. J. Comput. Dent.* **25**(3), 295–302 (2022).
12. Li, T. T. et al. Two-step strategy for constructing hierarchical pore structured chitosan-hydroxyapatite composite scaffolds for bone tissue engineering. *Carbohydr. Polym.* **15**(260), 117765 (2021).
13. Bolat, Ç. & Ergene, B. An investigation on dimensional accuracy of 3D printed PLA, PET-G and ABS samples with different layer heights. *Çukurova Üniversitesi Mühendislik Fakültesi Dergisi* **37**(2), 449–458 (2022).
14. Habib, A. A. I. & Sheikh, N. A. 3D printing review in numerous applications for dentistry. *J. Inst. Eng. India Ser. C* **103**, 991–1000 (2022).
15. Rungrojwittayakul, O. et al. Accuracy of 3D printed models created by two technologies of printers with different designs of model base. *J. Prosthodont.* **29**(2), 124–128 (2020).
16. Lai, Y. C. et al. The effects of additive manufacturing technologies and finish line designs on the trueness and dimensional stability of 3D-printed dies. *J. Prosthodont.* **32**(6), 519–526 (2023).
17. Park, J.-H. et al. Three-dimensional digital superimposition of orthodontic bracket position by using a computer-aided transfer jig system: An accuracy analysis. *Sensors (Basel, Switzerland)* **21**(17), 5911 (2021).
18. Park, J.-H. et al. Three-dimensional evaluation of the transfer accuracy of a bracket jig fabricated using computer-aided design and manufacturing to the anterior dentition: an in vitro study. *Korean J. Orthod.* **51**(6), 375–386 (2021).
19. Sherman, S. L., Kadioglu, O., Currier, G. E., Kierl, J. P. & Li, J. Accuracy of digital light processing printing of 3-dimensional dental models. *Am. J. Orthod. Dent. Orthop.* **157**(3), 422–428 (2020).
20. Hada, T. et al. Effect of printing direction on the accuracy of 3D-printed dentures using stereolithography technology. *Materials (Basel)* **13**(15), 3405 (2020).
21. Hada, T., Kanazawa, M., Iwaki, M., Arakida, T. & Minakuchi, S. Effect of printing direction on stress distortion of three-dimensional printed dentures using stereolithography technology. *J. Mech. Behav. Biomed. Mater.* **110**, 103949 (2020).
22. Topsakal, K. G., Gökmen, Ş., Yurdakurban, E., Duran, G. S. & Görgülü, S. The effect of layer thickness on the accuracy of the different in-house clear aligner attachments. *Clin. Oral Investig.* **27**(9), 5331–5341 (2023).
23. Hoffmann, L., Sabbagh, H., Wichelhaus, A. & Kessler, A. Bracket transfer accuracy with two different three-dimensional printed transfer trays vs silicone transfer trays. *Angle Orthod.* **92**(3), 364–371 (2022).
24. Grassia, V. et al. Accuracy (trueness and precision) of 3D printed orthodontic models finalized to clear aligners production, testing crowded and spaced dentition. *BMC Oral Health.* **23**(1), 352 (2023).
25. Unkovskiy, A. et al. Objects build orientation, positioning, and curing influence dimensional accuracy and flexural properties of stereolithographically printed resin. *Dent. Mater.* **34**(12), e324–e333 (2018).
26. Shim, J. S., Kim, J. E., Jeong, S. H., Choi, Y. J. & Ryu, J. J. Printing accuracy, mechanical properties, surface characteristics, and microbial adhesion of 3D-printed resins with various printing orientations. *J. Prosthet. Dent.* **124**(4), 468–475 (2020).
27. Arnold, C., Monsees, D., Hey, J. & Schweyen, R. Surface quality of 3D-printed models as a function of various printing parameters. *Materials (Basel)* **12**(12), 1970 (2019).
28. Castilla, A. E. et al. Measurement and comparison of bracket transfer accuracy of five indirect bonding techniques. *Angle Orthod.* **84**(4), 607–614 (2014).

Author contributions

FY Z: wrote the main manuscript text; MC H: concept and design of the study; YN C: extract data from the collected literature and analyze the data; LP Y, Z D, H M: search literature; YF G, XM F: have drafted the work or substantively revised it. All authors approved the final version of the manuscript. All persons named as authors warrant that they have reviewed and approved the manuscript prior to submission.

Funding

This work was supported by the Healthtalent plan of Taihu Lake in Wuxi (Double Hundred Medical Youth Professionals Program) from Health Committee of Wuxi (No. HB2023054). General Project of Wuxi Municipal Commission of Health and Family Planning (M202240). Clinical Research and Translational Medicine Research Program, Affiliated Hospital of Jiangnan University (LCYJ202223) (LCYJ202346). The funding bodies were not involved in the design of the study, data collection, analysis, or interpretation of the data and writing the manuscript.

Declarations

Competing interests

The authors declare no competing interests.

Ethics approval and consent to participate

Ethical approval was obtained from the Medical Ethics Committee, Affiliated Hospital of Jiangnan University in October 2022 (approval number: LS2022106). Written informed and oral consent was obtained from the study participants.

Additional information

Correspondence and requests for materials should be addressed to Y.G. or Y.C.

Reprints and permissions information is available at www.nature.com/reprints.

Publisher's note Springer Nature remains neutral with regard to jurisdictional claims in published maps and institutional affiliations.

Open Access This article is licensed under a Creative Commons Attribution-NonCommercial-NoDerivatives 4.0 International License, which permits any non-commercial use, sharing, distribution and reproduction in any medium or format, as long as you give appropriate credit to the original author(s) and the source, provide a link to the Creative Commons licence, and indicate if you modified the licensed material. You do not have permission under this licence to share adapted material derived from this article or parts of it. The images or other third party material in this article are included in the article's Creative Commons licence, unless indicated otherwise in a credit line to the material. If material is not included in the article's Creative Commons licence and your intended use is not permitted by statutory regulation or exceeds the permitted use, you will need to obtain permission directly from the copyright holder. To view a copy of this licence, visit <http://creativecommons.org/licenses/by-nc-nd/4.0/>.

© The Author(s) 2025